MICROCOPY RESOLUTION TEST CHART

NATIONAL BUREAU OF STANDARDS-1963-A

①

UNIVERSITY OF RHODE ISLAND

COLLEGE OF ENGINEERING

AD-A162 742

Annual Technical Report

~~Contract No. AFOSR-84-0205TEF~~

GRANT NO. AFOSR-83-0322

STUDY OF CRACK FRONT DISTRIBUTION DURING

CRACK PROPAGATION STAGE IN HIGH

PERFORMANCE ALLOYS

DTIC

ELECTE

DEC 30 1985

S   D

D

DEPARTMENT OF

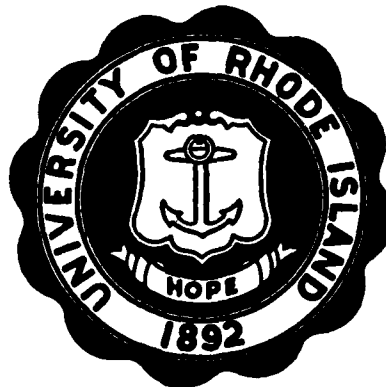# Mechanical Engineering and Applied Mechanics

KINGSTON, RHODE ISLAND 02881

85 12 30 035

8a. NAME OF FUNDING/SPONSORING ORGANIZATION AIR FORCE OFFICE OF SCIENTIFIC RESEARCH	8b. OFFICE SYMBOL (If applicable) AFOSR/NA	9. PROCUREMENT INSTRUMENT IDENTIFICATION NUMBER AOFSR-83-0322

8c. ADDRESS (City, State and ZIP Code) BOLLING AFB DC 20332-6448	10. SOURCE OF FUNDING NOS.			
	PROGRAM ELEMENT NO. 61102F	PROJECT NO. 2302	TASK NO. B2	WORK UNIT NO.

11. TITLE (Include Security Classification) "STUDY OF CRACKFRONT DISTRIBUTION DURING CRACK PROPAGATION" STAGE IN HIGH PERFORMANCE ALLOYS" (UNCLASSIFIED)

12. PERSONAL AUTHOR(S) GHONEM, HAMOUDA

13a. TYPE OF REPORT ANNUAL	13b. TIME COVERED FROM 15SEP83 TO 14SEP84	14. DATE OF REPORT (Yr., Mo., Day) 84 October 31	15. PAGE COUNT 45

16. SUPPLEMENTARY NOTATION

17. COSATI CODES			18. SUBJECT TERMS (Continue on reverse if necessary and identify by block number)
FIELD	GROUP	SUB. GR.	CRACK PROPAGATION STOCHASTIC MODEL
			CRACK GROWTH
			PROBABILISTIC CRACK GROWTH

19. ABSTRACT (Continue on reverse if necessary and identify by block number)

A stochastic model describing the crack evolution and scatter associated with the crack propagation process has been built on the basis of the discontinuous Markovian process. In this model the distributions of both the propagation life necessary to reach a specified crack length and the crack length at a specific number of cycles are derived in terms of constant probability crack growth curves. The significance of this model is that, by considering the crack growth curve obtained using any continuum model as being the mean growth curve, the present model is sufficient for the identification of the crack evolution and associated scatter without the necessity of performing scatter experiments. The validity of the model is established by compairing crack growth curves generated to Al 2024-T3 and Al 7075-T6 at specific loading conditions with those experimentally obtained and reported in literature. Emphasis is placed, during the development of the model, on its adherence to the physical aspects of the crack growth mechanism and the degree of agreement between theoretical results and corresponding experimental data.

20. DISTRIBUTION/AVAILABILITY OF ABSTRACT UNCLASSIFIED/UNLIMITED ☒ SAME AS RPT. ☐ DTIC USERS ☐	21. ABSTRACT SECURITY CLASSIFICATION UNCLASSIFIED

22a. NAME OF RESPONSIBLE INDIVIDUAL Dr Anthony K Amos	22b. TELEPHONE NUMBER (Include Area Code) 202/767-4937	22c. OFFICE SYMBOL AFOSR/NA

Annual Technical Report

~~Contract No. AFOSR-81-CE0312F~~

GRANT NO. AFOSR-83-0322

STUDY OF CRACK FRONT DISTRIBUTION DURING CRACK PROPAGATION STAGE IN HIGH PERFORMANCE ALLOYS

DTIC

S **ELECTE**

DEC 30 1985

D

D

by

Hamouda Ghonem
Associate Professor of Mechanical Engineering
University of Rhode Island
Kingston, RI   02881

Submitted to

Air Force Office of Scientific Research
Bolling Air Force Base, D.C.   20332

Table of Contents

Accesion For

NTIS CRA&I	✓
DTIC TAB	☐
Unannounced	☐
Justification	

By
Distribution/

Availability Codes

| Dist | Avail ard/or Special |
| A-1 | |

DTIG
COPY
INSPECTED
2

1. Summary

A stochastic model describing the crack evolution and scatter associated with the crack propagation process has been built on the basis of the discontinuous Markovian process. In this model the distributions of both the propagation life necessary to reach a specified crack length and the crack length at a specific number of cycles are derived in terms of constant probability crack growth curves. The significance of this model is that, by considering the crack growth curve obtained using any continuum model as being the mean growth curve, the present model is sufficient for the identification of the crack evolution and associated scatter without the necessity of performing scatter experiments. The validity of the model is established by comparing crack growth curves generated to Al 2024-T3 and Al 7075-T6 at specific loading conditions with those experimentally obtained and reported in literature. Emphasis is placed, during the development of the model, on its adherence to the physical aspects of the crack growth mechanism and the degree of agreement between theoretical results and corresponding experimental data.

2. Objectives

2.1 Theoretical

The major objective of this two years research program was to establish a quantitative model to describe the crack front evolution based on the fact that the crack growth is a stochastic discrete process where characteristics are influenced by the random nature of real polycrystalline solids. In the proposed model, which is based on the Markovian pure birth process, a transition intensity λ, was considered an important element in establishing the crack front distribution.

Here λ was assumed to depict the combined effects of the microstructure and loading parameters and was assumed to include a coupling factor to account for the strong nearest-neighbor-interaction related to the spatial distribution of conditional fracture states of points along the crack tip front. Obtaining an explicit expression for λ was thus an objective in the study.

2.2 Experimental

An experimental test program using a closed-loop servohydraulic testing system and a scanning electron microscope was proposed to study the fracture surface morphology. This would be assisted by a modified mapping technique capable of counting striations as well as measuring striations, spacings and excursions. This combined test procedure was proposed to provide an experimental description of the crack front and to generate the statistical data required for verifying the theoretical elements of the proposed theory. The experimental program was proposed to be carried out concurrently with the analytical development of the proposed theory and to be completed during the two year term of the research program.

3. Status of the Research (Period 09/15/83-09/15/84)

A model predicting evolution and scatter of the crack tip was established on the basis of the Markov process. While the model and efforts made to verify its concept are described in detail in Appendix I, the outline of the model and its results are as follows:

1. The model is based on the premises that scatter data of the crack growth process could be grouped to identify a family of crack lengths versus number-of-cycles curves, each of

which is a constant probability transition curve. The governing equation for such a cruve was developed as:

$$\ln P_r(i) = - B(e^{Ki} - e^{KI_0}) \qquad i \geq I_0$$

where $P_r(i)$ is the probability of the crack being at position r along the fracture surface after i cycles elapse; B and K are crack length dependent variables and I_0 is the minimum number of cycles required for the crack to advance from one position on the fracture surface to the next.

2. Using published data on the scatter of 68 replicate tests carried out on Al 2024-T3, the results were arranged to produce a family of crack lengths versus number-of-cycles curves. Each of these curves was constructed by joining growth lines of identical transition probability, P_r. In the present analysis eight curves were selected; their transition probabilities are: 0.95, 0.85, 0.72, 0.64, 0.50, 0.40, 0.20, and 0.10. The median, i.e. $P_r(i) = 0.5$ curve, which can be generated by the Paris-Erdagan Equation, was selected to provide information which would be used to derive the parameters B, K and I_0.

3. Using the constant probability equation, a set of theoretical curves corresponding to that obtained experimentally in step 2 was generated. Agreement between these two sets of curves was found to be in the range of 5%.

In addition to these major results, the concept of "incubation time" has been theoretically derived in this study. This concept, which identifies an absolute minimum time for the crack tip to advance from

one position to the following position, could be understood in terms of the crack tip threshold properties and could evolve as a critical element in the understanding of the crack growth mechanism.

4. Technical Publications

Three papers have been submitted to one journal and two conferences, they are:

1. Probabilistic Description of Fatigue Crack Growth in Poly-crystalline Solids. Accepted for publication in Int. J. of Engineering Fracture Mechanics.
   Authors: H. Ghonem and S. Dore

2. Crack Evolution and Scatter During Crack Propagation Stage in Polycrystalline Solids:
   Submitted to:

   - Structure, Structural Dynamics and Materials Conference, Orlando, FL, April 1985.
   - Reliability, Stress Analysis and Failure Prevention Conference, Cincinnati, Ohio, Sept. 1985

3. Critical Analysis of Probability Models for the Crack Growth Process. To be submitted to Int. J. of Engineering Fracture Mechanics.
   Authors: H. Ghonem and S. Dore.

Personnel Associated with the Research Efforts

Dr. H. Ghonem	Principal Investigator
Mr. S. Dore	Graduate Student
Mr. S. Grover	Graduate Student
Mr. H. Bui	Undergraduate Student

- Thesis expected to be finished April 1985

  Probabilistic Description of Fatigue Crack Growth in Polycrystalline

  Solids

- Recipient: S. Dore

    Degree: Masters of Mechanical Engineering

Appendix I

Probabilistic Description of Fatigue Crack
Growth in Polycrystalline Solids

INTRODUCTION

Laboratory tests conducted on different polycrystalline materials exhibited considerable variation in the crack growth characteristics data. This variation, or scatter, is considered a major factor in the gap that exists between theoretical predictions of existing continuum crack propagation models and experimental observations.

Several studies, employing theory of probability concepts, have been developed to predict and characterize the variation in crack propagation data. These studies generally follow two approaches. The first approach is based on the introduction of random variables encompassing the scatter sources to replace the deterministic parameters in continuum crack propagation rules such as the Paris-Erdogan Equation (1) which is widely studied and used. The result of this operation is viewed as a sample crack growth equation by which mean crack position and associated variance can be calculated. Examples of models belonging to this approach are those of Hoeppner and Krupp (2), Gurney (3), Ostergaard and Hillberry (4) and others (5-7).

The second approach is based on the assumption that the crack propagation process could be formulated in terms of a particular discontinuous Markovian process. This leads to the description of the crack length in the form of its probability distribution whose evolution in time characterizes the non-deterministic nature of the crack propagation process. Examples of these models are found in the work of Ghonem and Provan (8) and Bogdanoff and Kozin (9).

This paper is an attempt to extend the concepts presented in Ref. (8) to produce a theoretical method which will estimate the

crack growth scatter at any stress level. This is achieved by developing the sample functions of the crack growth process in terms of a constant-probability crack growth criterion. Mathematical elements of this criterion are detailed in the first part of this paper while the second part deals with the use of the model in a numerical example to estimate crack growth scatter in Aluminum 2024-T3. Emphasis is placed on the adherence of the model to the physical aspects of the crack growth process and the degree of agreement between the theoretical results of the model and corresponding experimental data.

MATHEMATICAL ELEMENTS OF THE MODEL

The stochastic model of the fatigue crack propagation as briefly described in (8) is developed in terms of a general pure birth, discontinuous Markovian stochastic process. The model is based on the assumption that the crack front can be approximated, as shown in Figure 1, by a large number of elements α, $\alpha = 1,...,M$, each of which, in terms of the theory of probability, identifies a statistical trial or experiment. The fracture state of the αth trial at cycle i is given by the crack length or the random variable $^{\alpha}a_i$ whose evolution with time shall then be established. $^{\alpha}a_i$ will hereafter be referred to as a_i.

Due to the built-in limitations of all experimental techniques the observed value of a_i can only be specified within the range of:

$$x < a_i < x + \Delta x \tag{1}$$

where Δx is the experimental error and x is the crack position cal-

culated as (see Figure 2):

$$x = r \, \Delta x \qquad\qquad ; \; r_0 < r < r_f \qquad (2)$$

Here r identifies the observable zone or state along the fracture surface; r_0 is the initial propagation state, r_f is the state just prior to catastrophic failure of the specimen and r_1, r_2,...r_{f-1} are the intermediate zones.

Given that the crack is in state r, then after i cycles have elapsed from the instant of reaching r, one of two events would occur; a_i would remain in state r (event $^r E_i$) or a_i would not be in state r (event $^s E_i$). The following observations can now be made:

1- Due to the fact that the propagation process is an irreversible one, the crack, if it does not stay in r, must exist in a state greater than r.

2- Since it is not possible for the crack to propagate from one state to any other state without penetrating the immediate neighboring state, each crack could then be identified by the number of cycles required to advance from a given state to the following one.

Based on these observations the two events $^r E_i$ and $^s E_i$ can be seen as the element of a measurable sample space Ω, see Ref. (9), and the following definition of the probability measure of a_i becomes possible. At any fatigue cycle i the probability that a_i is in state r, i.e. the probability of $^r E_i$, is defined as:

$$P \{a_i \in {}^r E_i \} = P \{x < a_i < x + \Delta x \}$$

$$\text{i.e.} \quad P(^{r}E_{i}) = P_{r}(i) \tag{3}$$

Therefore the probability of a_i not falling within r is

$$P(^{S}E_{i}) = P_{S}(i) = 1 - P_{r}(i) \tag{4}$$

Here $P_{S}(i)$ continuously increases as the number of cycles increase.

Furthermore, it is known that the existence of the crack front at a particular position inside the material depends on its present mechanical and microstructure details and is not directly influenced by the details of any of its other previous positions. More specifically, the probability of a_i propagating from state r to r+1 in the cycle interval $(i, i+\Delta i)$ depends on the event $^{r}E_{i}$ and is independent of any event $^{q}E_{j}, \ldots, ^{P}E_{0}$ occurring prior to i; $0 < j < i$. This can be expressed as:

$$P \{^{t}E_{\Delta i}/^{r}E_{i}, \ldots, ^{q}E_{j}, \ldots, ^{P}E_{0}\} = P \{^{t}E_{\Delta i}/^{r}E_{i}\} \tag{5}$$

where $t = r+1$ and '/' denotes a conditional probability measure. These characteristics together with the evolution of a_i within the two-event space Ω, describe a discontinuous Markovian process. The function $P_{rt}(i)$ could then be considered the transition probability linking the probability measures of two consecutive states r and t; $t = r+1$, along the fracture surface.

It is now possible to describe the propagation process of the crack front in terms of the following criteria:

1- The probability of a_i propagating to a state different than r in Δi cycles is given by

$$P_s(\Delta i) = P\{^{r+1}E_{\Delta i} / {}^rE_i\} + 0(\Delta i)$$

$$= \lambda_r \, \Delta i + 0(\Delta i) \tag{6}$$

where λ_r is a positive parameter describing the crack transition rate from state r to t in Δi cycles and is thus considered a material- and time-dependent variable, see Bharucha-Reid (11).

2- The corresponding probability that a_i will be in state r during the cycle interval Δi is:

$$P_r(\Delta i) = P\{^rE_{\Delta i} / {}^rE_i\} + 0 \, (\Delta i)$$

$$= (1 - \lambda_r \, \Delta i) + 0 \, (\Delta i) \tag{7}$$

3- The probability that a_i is in a state different from r+1 is:

$$P_{rt}(\Delta i) = P\{^tE_{\Delta i} / {}^rE_i\}$$

$$= 0 \, (\Delta i) \qquad\qquad ; \; t > r+1 \tag{8}$$

Since

$$P\{^rE_{i+\Delta i}\} = P\{^rE_{\Delta i} / {}^rE_i\} \cdot P\{^rE_i\} \tag{9}$$

Therefore substituting Equations 6, 7 and 8 in Equation 9, the probability of the event $^rE_{\Delta i}$ can be obtained as:

$$P_r(i+\Delta i) = (1 - \lambda_r \, \Delta i) \, P_r(i) + 0 \, (\Delta i) \tag{10}$$

By transposing and taking the limit $\Delta i \to 0$, Equation (10) becomes:

$$\frac{dP_r(i)}{di} = - \lambda_r \, P_r(i) \tag{11}$$

The solution of this equation is:

$$\ell n \, P_r(i) = - \int \lambda_r \, di + C_1 \tag{12}$$

where C_1 is a constant.

An important element in solving this equation is the parameter λ_r which is seen here as a measure of the crack growth rate. This measure is assumed to have the following properties:

1- In the presence of continuous cyclic loading the longer the cycle duration during which the crack is in a specific state, the higher the probability that the propagation threshold of the crack tip is satisfied and the higher the probability that the crack will advance. This indicates that in a general case, λ_r increases monotonically with an increase in the number of cycles i

2- λ_r being a material-dependent variable should then possess a non-zero positive value at cycle i = 0

Based on these observations λ_r is chosen to have the following form:

$$\lambda_r = C_2 \, e^{Ki} \tag{13}$$

where C_2 and K are crack-position dependent and time dependent parameters. Substituting (13) in (12) one obtains

$$\ell n\ P_r(i) = -B\ e^{Ki} + C_1 \qquad (14)$$

where

$$B = \frac{C_2}{K}$$

Upper and lower limits of $P_r(i)$ in the above equation are

$$1 \geq P_r(i) \geq 0$$

The form of Equation (14) suggests that i has a lower boundary which satisfies the upper limit of $P^r(i)$. This means that Equation (14) will be valid only for $i \geq I_0$ where I_0 is the lower boundary of i or simply the minimum number of cycles required for the crack to advance from state r. In this approach, concepts such as those of the weakest-link theory by Weibull (12) and others (13,14) have not been taken into consideration. Hence, the upper limit condition for $P_r(i)$ can be expressed as:

$$P_r(i) = 1 \qquad ; \quad i < I_0$$

By invoking this upper limit condition on Equation (14) the constant C_1 is obtained as

$$C_1 = B \, e^{KI_0} \qquad (15)$$

Equation (14) could then be written in the form:

$$P_r(i) = e^{B(e^{KI_0} - e^{Ki})} \qquad ; \quad i \geq I_0$$

$$\qquad (16)$$

$$P_r(i) = 1 \qquad ; \quad i < I_0$$

This result, illustrated in Figure 3, describes a set of curves which can be obtained by varying $P_r(i)$. Each of these curves is a constant probability curve identifying the discrete crack position and the corresponding number of cycles. Since the variables B, K and I_0 are functions of the crack length, they are related to the crack length through certain constants. These constants can be determined by using one known constant probability crack growth curve and Equation (16) consequently becomes fully defined. The significance of this concept is that if the crack growth curve obtained by using a continuum model is considered as being the mean growth curve, i.e., the $P_r(i) = 0.5$ curve, a view that is consistent with the application of the majority of the continuum models, the parameters B, K and I_0 can then be calculated and Equation (16) becomes sufficient to identify the crack length and associated scatter in number of cycles at any stress level without the need to perform scatter experiments. In the next part of the paper this model will be employed in a numerical example to estimate the crack growth curves of Aluminum 2024-T3 and results will be compared to available experimental data.

APPLICATION

The first step to be dealt with here is the determination of the unknown variables B, K and I_0 in Equation (16). To achieve this the authors utilized experimental crack growth scatter data obtained by Virkler, Hillberry and Goel (15) and Yang, Donath and Salivar (16).

The first set of data (15) is obtained from 68 identically prepared Aluminum 2024-T3 tension specimens with a central slot perpendicular to the loading axis. The data consists of the number of cycles necessary to reach the same specified crack length for each specimen; 164 crack lengths are recorded ranging from 9 mm to 49.8 mm for a half crack length. The 68 sample crack growth curves are shown in Figure 4. These curves were utilized to obtain constant probability crack growth curves as follows: The total crack length was divided into 204 states; each with a width of 0.2 mm. The number of cycles spent in each state was calculated and arranged in ascending order; the largest number was assigned a probability of:

$$P_r(i) = 1 - (x/68) \qquad ; x = 68$$

and so on, up to a probability of:

$$P_r(i) = 1 - (x/68) \qquad ; x = 1$$

for the shortest number of cycles. Points with equal probability were connected and a set of ten constant probability curves was generated as shown in Figure 5. Data points representing the number

of cycles corresponding to similar discrete crack positions along three different constant probability growth curves, $P_r(i) = 0.5$, 0.50 and 0.95, where used as input for Equation (16) to determine the variables B, K and I_0. The values obtained are listed in Table (1). These values are plotted versus the crack length position i.e. state r in Figure 6(a, b and c); and by using regression analysis the following relationships were constructed.

$$B = 0.018 \; r^{0.28}$$

$$K = 2.498 \times 10^{-7} \; r^{1.95} \tag{17}$$

$$I_0 = 0.94 \times 10^7 \; [(r-1)^{-1.01} - r^{-1.01}]$$

To confirm these relationships, another set of crack growth scatter data of IN 100, a superalloy used in certain gas turbine engines, was used (16). The data consisted of the distribution of crack size as function of load cycles for 2 different load conditions as shown in Figs. 7(a,b). Analysis similar to that done on the work of Virkler and co-workers was carried out, yielding two sets of values for B, K and I_0. They are shown in Table (2). These values are again plotted vs the crack length position as shown in Figs. 8(a,b,c) and 9(a,b,c) and the following relationships were obtained.

Test Condition I

$$B = 0.055 \; r^{0.76}$$

$$K = 1.362 \times 10^{-6} \; r^{2.34} \tag{18}$$

$$I_0 = 2.743 \times 10^5 \; [(r-1)^{-0.71} - r^{-0.71}]$$

Test Condition II

$$B = 0.059 \, r^{0.73}$$

$$K = 6.68 \times 10^{-7} \, r^{2.015}$$

$$I_0 = 1.843 \times 10^6 [(r-1)^{-1.45} - r^{-1.45}]$$

By observing Equations (17), (18), (19) general forms of B, K and I_0 in terms of crack length a, could be written as

$$B = C_1 \, a^{n_1}$$

$$K = C_2 \, a^{n_2} \qquad\qquad (20)$$

$$I_0 = C_3 [(a - x)^{n_3} - a^{n_3}]$$

An attempt can now be made using Equation (16) in conjunction with Equation (20) to generate constant probability curves for the test conditions of Virkler et al (15). These curves could then be compared to those experimentally obtained in Figure 5. The first step is to obtain the mean crack growth curve utilizing, as mentioned before, a continuum crack growth equation. In this application the Paris-Erdogan Equation in the following form is used to generate such a curve:

$$\Delta i = \frac{1}{C(\Delta\sigma \sqrt{\pi})^n} \frac{1}{m-1} [a_0^{1-m} - a_f^{1-m}]; \; m = \frac{n}{2} \qquad (21)$$

for Al 2024-T3 the index n is equal to 4 while the parameter C attains values ranging from 3.5×10^{-10} to 3.79×10^{-10}. Equation (21) was then

used to obtain the crack growth curve as shown in Figure 10 (C = 3.79 x 10^{-10}, a_o = 9 mm and $\Delta\sigma$ = Ksi). This curve is viewed here as equivalent to the experimental mean curve, i.e. the $P_r(i)$ = 0.5 curve.

The number of cycles corresponding to six discrete crack positions along the Paris-Erdogan curve was then used as input for Equations (16) and (20) where $P_r(i)$ = 0.5. These six equations were solved by an iterative technique employing Newton-Raphson's method. Converging values for the six constants were found as followes:

$$C_1 = 0.0563 \qquad C_2 = 2.04 \times 10^{-7} \qquad C_3 = 1.022 \times 10^{-7}$$

$$n_1 = 0.298 \qquad n_2 = 1.917 \qquad n_3 = -1.0$$

Making use of these constants, Equations (16) and (20) were again utilized to generate a set of theoretical constant-probability crack growth curves as shown in Figure 11. These curves were compared to those experimentally obtained in Figure 5 and results of this comparison in the form of percentage of error of number of cycles corresponding to similar crack lengths are listed in Table 3 and summarized in Figure 12. On the basis of these results the following observations can be made:

1- The present model succeeds in describing the evolution of the crack growth by estimating the number of cycles required for the crack to advance from one discrete position along the fracture surface to the following one. The evolution process was carried out for constant-probability crack growth curves. From these curves the scatter in the crack length at a specific fatigue

as well as the scatter in the number of cycles required to advance the crack to a specific length, can be estimated. The results of the model, when applied to Al 2024-T3 that have been subjected to fatigue cycles with a constant stress amplitude, are in agreement with those experimentally obtained. Average error in the theoretical curves is estimated to be 5% which is within the scatter limit of any experimental curve. The accuracy of the model, however, seems to depend on the degree of agreement between the crack growth curve obtained using a continuum theory and the experimental mean curve. To examine this effect in the present application, the value of the parameter C in the Paris-Erdogan Equation was changed from 3.79×10^{-10} to 3.51×10^{-10} so that the deviation of the theoretical mean curve from the experimental one is increased as shown in Figure 10. As a result the average error in the prediction of the model, as illustrated in Figure 12, is increased from 5% to 13%.

2- The degree of scatter in the number of cycles corresponding to a specified state is observed to decrease as the crack length increases. At higher crack lengths all the cracks require about the same number of cycles to advance from one discrete position to the following one. This may then lead to the conclusion that the degree of scatter in the number of cycles to failure depends on the large scatter observed in the early stages of crack propagation. This is illustrated in Figure 14. The effect of scatter associated with "short" cracks on the variation in the number of cycles required for the crack to reach a critical length is currently under investigation by the authors.

3- The notion that there is a minimum number of cycles required for the crack to advance from one position on the fracture surface to the next

immediate one has been theoretically derived in this model through the parameter I_o in Equation (16). This concept of "incubation time" could be interpreted in relation to the time required for the crack tip propagation threshold (such as a specified mobile dislocation density, a thermodynamic activation level or any other criterion) to be satisfied. This concept warrants further study.

CONCLUDING REMARK

A model is presented here describing the crack propagation process as a discontinuous Markovian process. Based on this, the concept of constant-probability crack growth curves has been quantitatively derived. With the assumption that the crack growth curve given by any continuum crack growth model coincides with the experimental mean growth curve the proposed model has demonstrated that it could sufficiently describe the evolution of the crack length and associated scatter at any stress level.

REFERENCES

1. Paris, P. and Erdogan, F., "A Critical Analysis of Crack Propagation Law," Journal of Basic Engineering, Trans. ASME, Series D. Vol. 85, December 1963.

2. Hoeppner, D.W. and Krupp, W.E., "Prediction of Component Life by Application of Fatigue Crack Growth Knowledge," Engineering

Fracture Mechanics, Vol. 6, 1974.

3. Gurney, T.R., "Fatigue of Welded Structures," Cambridge University Press, 1979.

4. Ostergaard, D.F. and Hillberry, B.M., "Characterization of the Variability in Fatigue Crack Propagation Data," Probabilistic Fracture Mechanics and Fatigue Methods: Application for Structural Design and Maintenance, ASTM STP798, J.M. Bloom and J.C. Ekvall, Eds., ASTM, 1983, pp. 97-115.

5. Johnston, G.O., "Statistical Scatter in Fracture Toughness and Fatigue Growth Rate Data," Probabilistic Fracture Mechanics and Fatigue Methods: Applications for Structural Design and Maintenance, ASTM STP798, J.M. Bloom and J.C. Ekvall, Eds., ASTM 1983, pp. 42-66.

6. McCartney, L.N. and Cooper, P.M., "A New Method of Analyzing Fatigue Crack Propagation Data," Engineering Fracture Mechanics, Vol. 9, No. 2, 1977.

7. Forman, R.G., Kearney, V.E. and Engle, R.M., "Numerical Analysis of Crack Propagation in Cyclic-Loaded Structures," Journal of Basic Engineering, Series D, Vol. 89, 1967.

8. Ghonem, H. and Provan, J.M., "Micromechanics Theory of Fatigue Crack Initiation and Propagation," Engineering Fracture Mechanics, Vol. 13, No. 4, 1980.

9. Kozin, F. and Bogdanoff, J.L., "A Critical Analysis of Some Probabilistic Models of Fatigue Crack Growth," Engineering Fracture Mechanics, Vol. 14, 1981.

10. Ghonem, H., "Stochastic Fatigue Crack Initiation and Propagation

in Polycrystalline Solids," Ph.D. Thesis, McGill University, 1978.

11. Bharucha-Reid, A.T., "Elements of the Theory of Markov Processes and its Applications," McGraw-Hill, New York, 1960.

12. Weibull, W., "A Statistical Theory of the Strength of Materials," Ing. Vetenskaps Hkad. Handl., No. 151, 1939.

13. Oh, K.P., "A Weakest-Link Model for the Prediction of Fatigue Crack Growth Rate," ASME Journal of Engineering Materials and Technology, Vol. 100, April 1978.

14. Tsurui, A. and Igarashi, A., "A Probabilistic Approach to Fatigue Crack Growth Rate," ASME Journal of Engineering Materials and Technology, Vol. 102, July 1980.

15. Virkler, D.A., Hillberry, B.M. and Goel, P.K., "The Statistical Nature of Fatigue Crack Propagation," ASME Journal of Engineering Materials and Technology, Vol. 101, April 1979.

16. Yang, J.N., Donath, R.C. and Salivar, G.C., "Statistical Fatigue Crack Propagation of IN 100 at Elevated Temperatures," ASME Int. Conf. on Advances in Life Prediction Methods, Albany, N.Y., April 18-20, 1983.

Crack Length Position r	I_o (cycles)	B ($\times 10^{-2}$)	K ($\times 10^{-3}$)
55	3166	5.5	0.617
65	2269	5.8	0.856
75	1706	6.0	1.133
85	1330	6.2	1.446
95	1066	6.4	1.796
105	873	6.6	2.183
115	729	6.8	2.604
125	618	6.9	3.063
135	530	7.1	3.555
145	460	7.2	4.086
155	403	7.3	4.647
165	356	7.5	5.249
175	317	7.6	5.885
185	283	7.7	6.549
195	255	7.8	7.249
205	231	8.0	7.984
215	210	8.1	8.751
225	192	8.2	9.547
235	176	8.3	11.040
245	162	8.4	11.127

Table 1: Values of B, K and I_0 for Different Crack Length Position r (Δx = 0.2 mm)

TEST CONDITION I

Crack Length Position	I_0 (cycles)	B ($\times 10^{-1}$)	K ($\times 10^{-4}$)
6	10280	1.915	0.946
7	8036	2.715	1.117
8	7203	2.836	1.719
9	5460	3.014	2.144
10	4169	3.143	3.206
11	3387	3.263	3.777
12	2806	3.518	4.407
13	2326	3.981	5.150

TEST CONDITION II

Crack Length Position	I_0 (cycles)	B ($\times 10^{-1}$)	K ($\times 10^{-4}$)
6	39940	2.189	0.268
7	28870	2.423	0.334
8	24050	2.688	0.4273
9	14410	2.998	0.4675
10	9275	3.228	0.692
11	7618	3.308	1.014
12	6402	3.637	1.017
13	5704	3.834	1.136

Table 2: Values of B, K and I_0 for Different Crack Length Positions (Δx = 0.1 in)

P = 0.897

STATE	NO. CYCLES (EXPTL.)	NO. CYCLES (THEOR.)	% ERROR
46	5529.0	5335.0	3.509
47	10749.0	10443.0	2.847
48	15793.0	15338.0	2.881
49	20480.0	20033.0	2.183
50	24835.0	24540.0	1.188
51	28920.0	28870.0	0.173
52	32960.0	33034.0	0.225
53	36747.0	37040.0	0.797
54	40317.0	40898.0	1.441
55	43763.0	44615.0	1.947
56	47090.0	48199.0	2.355
57	50288.0	51658.0	2.724
58	53443.0	54997.0	2.908
59	56236.0	58223.0	3.533
60	58971.0	61341.0	4.019
70	81344.0	87617.0	7.712
80	97397.0	107316.0	10.184
90	110576.0	122630.0	10.901
100	122030.0	134876.0	10.527
110	131667.0	144893.0	10.045
120	140420.6	153235.0	9.126
130	147991.0	160292.0	8.312
140	155049.0	166336.0	7.280
150	161046.0	171573.0	6.537
160	166576.0	176155.0	5.751
170	171394.0	180194.0	5.134
180	175477.0	183796.0	4.735
190	179242.5	186997.0	4.326
200	182494.0	189885.0	4.050
210	185287.0	192497.0	3.891
220	187594.0	194872.0	3.880
230	189482.5	197037.0	3.987
240	190995.3	199022.0	4.203

P = 0.838

STATE	NO. CYCLES (EXPTL.)	NO. CYCLES (THEOR.)	% ERROR
46	5911.0	5550.0	6.107
47	11431.0	10864.0	4.960
48	16613.0	15956.0	3.955
49	21586.0	20840.0	3.456
50	26298.0	25529.0	2.924
51	30750.0	30034.0	2.328
52	35030.0	34365.0	1.898
53	39005.0	38532.0	1.213
54	42789.0	42545.0	0.570
55	46302.0	46412.0	0.238
56	49656.0	50140.0	0.975
57	52896.0	53738.0	1.592
58	56129.0	57211.0	1.928
59	59174.0	60566.0	2.352
60	62037.0	63809.0	2.856
70	86113.0	91137.0	5.834
80	103634.0	111621.0	7.707
90	117827.0	127540.0	8.243
100	129916.0	140269.0	7.969
110	140358.0	150676.0	7.351
120	149576.6	159344.0	6.530
130	157713.0	166674.0	5.682
140	165122.0	172952.0	4.742
150	171606.0	178392.0	3.954
160	177447.0	183147.0	3.212
170	182531.0	187341.0	2.635
180	186888.5	191067.0	2.236
190	190881.5	194399.0	1.843
200	194329.0	197396.0	1.578
210	197308.5	200106.0	1.418
220	199733.5	202568.0	1.419
230	201686.0	204818.0	1.553
240	203290.3	206876.0	1.764

P = 0.750

STATE	NO. CYCLES (EXPTL.)	NO. CYCLES (THEOR.)	% ERROR
46	6232.0	5873.0	5.761
47	12183.0	11495.0	5.647
48	17782.0	16883.0	5.056
49	22953.0	22051.0	3.930
50	27806.0	27012.0	2.855
51	32530.0	31778.0	2.312
52	36957.0	36360.0	1.615
53	41217.0	40769.0	1.087
54	45166.0	45013.0	0.344
55	48858.0	49106.0	0.508
56	52402.0	53090.0	1.237
57	55937.0	54856.0	1.643
58	59322.0	60530.0	2.036
59	62616.0	64080.0	2.338
60	65646.0	67511.0	2.841
70	91434.0	96417.0	5.450
80	110266.0	118080.0	7.086
90	125616.0	134914.0	7.402
100	138682.0	148370.0	6.986
110	149920.0	159370.0	6.303
120	159779.0	168528.0	5.476
130	168564.0	176270.0	4.572
140	176448.0	182901.0	3.657
150	183346.0	188645.0	2.890
160	189547.0	193667.0	2.174
170	195017.0	198095.0	1.578
180	199731.0	202028.0	1.150
190	203948.0	205543.0	0.782
200	207702.0	208705.0	0.483
210	210858.0	211565.0	0.335
220	213446.0	214162.0	0.335
230	215517.5	216534.0	0.472
240	217205.8	218706.0	0.691

Table 3: Percentage Error Between the Theoretical and Experimental Constant-Probability Crack Growth Curves

P= 0.647

STATE	NO. CYCLES (EXPTL.)	NO. CYCLES (THEOR.)	% ERROR
46	6579.0	6256.0	4.910
47	12820.0	12246.0	4.477
48	18582.0	17986.0	3.207
49	24079.0	23491.0	2.442
50	29117.0	28776.0	1.171
51	34140.0	33853.0	0.841
52	38760.0	38735.0	0.064
53	43316.0	43432.0	0.268
54	47444.0	47955.0	1.077
55	51371.0	52313.0	1.834
56	55167.0	56515.0	2.443
57	58831.0	60570.0	2.956
58	62333.0	64484.0	3.451
59	65881.0	68265.0	3.619
60	69102.0	71920.0	4.078
70	96499.0	102712.0	6.438
80	116986.0	125785.0	7.521
90	133386.0	143714.0	7.743
100	147313.0	158042.0	7.283
110	159244.0	169753.0	6.599
120	169732.6	179502.0	5.756
130	179030.0	187743.0	4.867
140	187308.0	194801.0	4.000
150	194553.0	200912.0	3.269
160	201128.0	206253.0	2.548
170	206875.0	210963.0	1.976
180	211880.0	215146.0	1.541
190	216421.5	218887.0	1.139
200	220380.5	222250.0	0.849
210	223699.5	225290.0	0.711
220	226445.0	228052.0	0.710
230	228605.3	230571.0	0.860
240	230391.5	232881.0	1.081

P= 0.500

STATE	NO. CYCLES (EXPTL.)	NO. CYCLES (THEOR.)	% ERROR
46	7160.0	6831.0	4.595
47	13764.0	13371.0	2.855
48	19944.0	19638.0	1.534
49	25805.0	25650.0	0.601
50	31221.0	31421.0	0.641
51	36398.0	36965.0	1.558
52	41237.0	42296.0	2.568
53	45970.0	47426.0	3.167
54	50394.0	52365.0	3.911
55	54558.0	57125.0	4.705
56	58504.0	61714.0	5.487
57	62310.0	66142.0	6.150
58	66045.0	70417.0	6.620
59	69760.0	74547.0	6.862
60	73251.0	78539.0	7.219
70	103215.0	112173.0	8.679
80	125695.0	137375.0	9.292
90	143921.0	156958.0	9.058
100	159193.0	172607.0	8.426
110	171894.0	185398.0	7.856
120	183197.0	196047.0	7.014
130	193126.0	205046.0	6.172
140	201932.0	212752.0	5.358
150	209728.0	219423.0	4.624
160	216804.0	225256.0	3.898
170	222998.0	230397.0	3.318
180	228413.0	234962.0	2.867
190	233200.5	239045.0	2.506
200	237419.0	242716.0	2.231
210	240980.5	246034.0	2.097
220	243921.0	249047.0	2.102
230	246261.5	251797.0	2.248
240	248183.0	254314.0	2.470

P= 0.352

STATE	NO. CYCLES (EXPTL.)	NO. CYCLES (THEOR.)	% ERROR
46	7586.0	7475.0	1.463
47	14513.0	14633.0	0.827
48	20966.0	21493.0	2.514
49	27321.0	28073.0	2.752
50	33093.0	34390.0	3.919
51	38486.0	40459.0	5.127
52	43649.0	46295.0	6.062
53	48680.0	51911.0	6.637
54	53460.0	57319.0	7.218
55	58000.0	62530.0	7.810
56	62311.0	67555.0	8.416
57	66383.0	72404.0	9.070
58	70384.0	77085.0	9.521
59	74221.0	81608.0	9.953
60	77907.0	85980.0	10.362
70	110375.0	122818.0	11.273
80	135245.0	150428.0	11.226
90	155181.0	171885.0	10.764
100	171665.0	189033.0	10.117
110	185504.0	203051.0	9.459
120	197615.6	214723.0	8.657
130	208376.0	224589.0	7.781
140	217928.0	233037.0	6.933
150	226365.0	240353.0	6.179
160	234018.0	246749.0	5.440
170	240733.0	252386.0	4.841
180	246708.0	257392.0	4.331
190	251879.5	261869.0	3.966
200	256352.5	265893.0	3.722
210	260165.5	269530.0	3.599
220	263334.5	272836.0	3.608
230	265885.8	275850.0	3.748
240	267913.5	278611.0	3.993

Table 3: Continued

P= 0.250

STATE	NO. CYCLES (EXPTL.)	NO. CYCLES (THEOR.)	% ERROR
46	8047.0	7998.0	0.609
47	15345.0	15657.0	2.033
48	22089.0	22997.0	4.111
49	28870.0	30038.0	4.046
50	34921.0	36798.0	5.375
51	40582.0	43294.0	6.683
52	45899.0	49540.0	7.933
53	51080.0	55551.0	8.753
54	55957.0	61339.0	9.618
55	60664.0	66917.0	10.308
56	65207.0	72296.0	10.872
57	69555.0	77487.0	11.404
58	73856.0	82499.0	11.703
59	77969.0	87341.0	12.020
60	81932.0	92021.0	12.314
70	116421.0	131469.0	12.926
80	144055.0	161043.0	11.793
90	165539.0	184032.0	11.171
100	183301.0	202410.0	10.425
110	198092.0	217437.0	9.766
120	211008.0	229949.0	8.976
130	222459.0	240528.0	8.122
140	232461.0	249586.0	7.367
150	241368.0	257430.0	6.655
160	249507.0	264289.0	5.924
170	256701.0	270335.0	5.311
180	263152.0	275704.0	4.770
190	268602.5	280505.0	4.431
200	273347.0	284821.0	4.198
210	277386.0	288724.0	4.087
220	280749.5	292269.0	4.103
230	283435.5	295505.0	4.258
240	285613.3	298467.0	4.500

P= 0.162

STATE	NO. CYCLES (EXPTL.)	NO. CYCLES (THEOR.)	% ERROR
46	8437.0	8556.0	1.410
47	16265.0	16750.0	2.982
48	23271.0	24604.0	5.728
49	30384.0	32138.0	5.773
50	37031.0	39372.0	6.322
51	42961.0	46323.0	7.826
52	48452.0	53008.0	9.403
53	53908.0	59441.0	10.264
54	59080.0	65637.0	11.099
55	64060.0	71608.0	11.783
56	68843.0	77366.0	12.380
57	73448.0	82922.0	12.899
58	77883.0	88287.0	13.358
59	82187.0	93471.0	13.730
60	86420.0	98482.0	13.957
70	123298.0	140727.0	14.136
80	153285.0	172411.0	12.477
90	176432.0	197049.0	11.686
100	195702.0	216750.0	10.755
110	211331.5	232861.0	10.188
120	225042.0	246280.0	9.437
130	237197.0	257627.0	8.613
140	247745.0	267346.0	7.912
150	257164.0	275763.0	7.232
160	265905.0	283123.0	6.475
170	273669.0	289610.0	5.825
180	280612.0	295374.0	5.261
190	286401.0	300527.0	4.932
200	291373.5	305160.0	4.732
210	295646.5	309352.0	4.636
220	299187.5	313158.0	4.669
230	302099.3	316631.0	4.810
240	304475.8	319813.0	5.037

P= 0.103

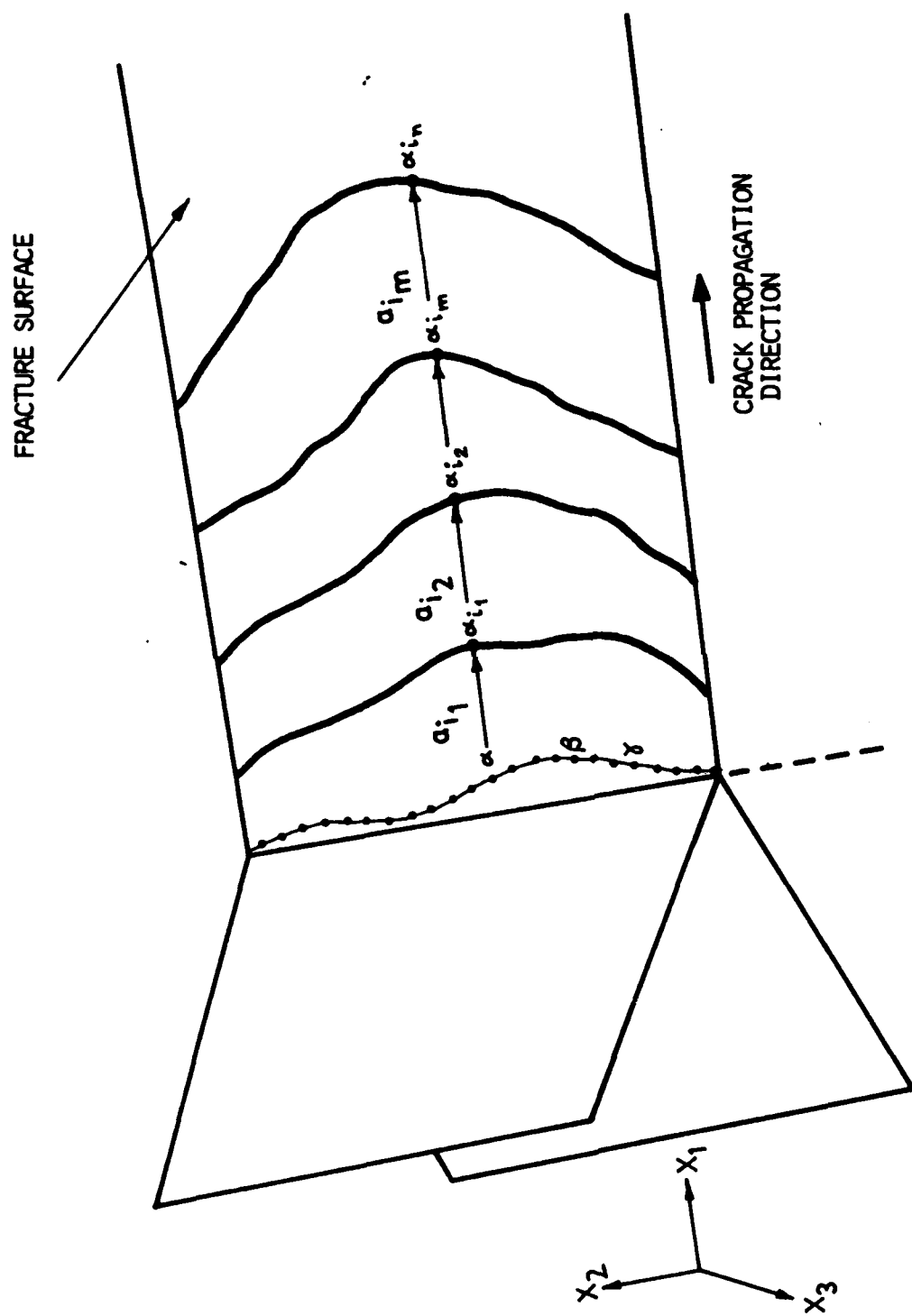| STATE	NO. CYCLES (EXPTL.)	NO. CYCLES (THEOR.)	% ERROR
46	8502.0	9050.0	6.446
47	16529.0	17717.0	7.187
48	23857.0	26023.0	9.087
49	31390.0	33995.0	8.299
50	38368.0	41648.0	8.549
51	44584.0	49002.0	9.909
52	50336.0	56075.0	11.401
53	55989.0	62882.0	12.311
54	61362.0	69438.0	13.161
55	66759.0	75756.0	13.477
56	71817.0	81849.0	13.969
57	76952.0	87729.0	14.005
58	81593.0	93407.0	14.479
59	86233.0	98893.0	14.681
60	90577.0	104197.0	15.037
70	129977.0	148919.0	14.573
80	162330.0	182477.0	12.411
90	187094.0	208577.0	11.482
100	207907.0	229452.0	10.363
110	224661.0	246528.0	9.733
120	239112.0	260753.0	9.051
130	251969.0	272785.0	8.261
140	263055.0	283094.0	7.618
150	273014.0	292022.0	6.962
160	282229.0	299829.0	6.236
170	290501.0	306713.0	5.581
180	297894.0	312830.0	5.014
190	304104.0	318300.0	4.668
200	309289.5	323218.0	4.503
210	313773.5	327666.0	4.428
220	317566.5	331706.0	4.452
230	320624.3	335393.0	4.606
240	323183.8	338770.0	4.823

Table 3: Continued

Figure 1: Schematic of Mode I Crack Propagation Fracture Surface
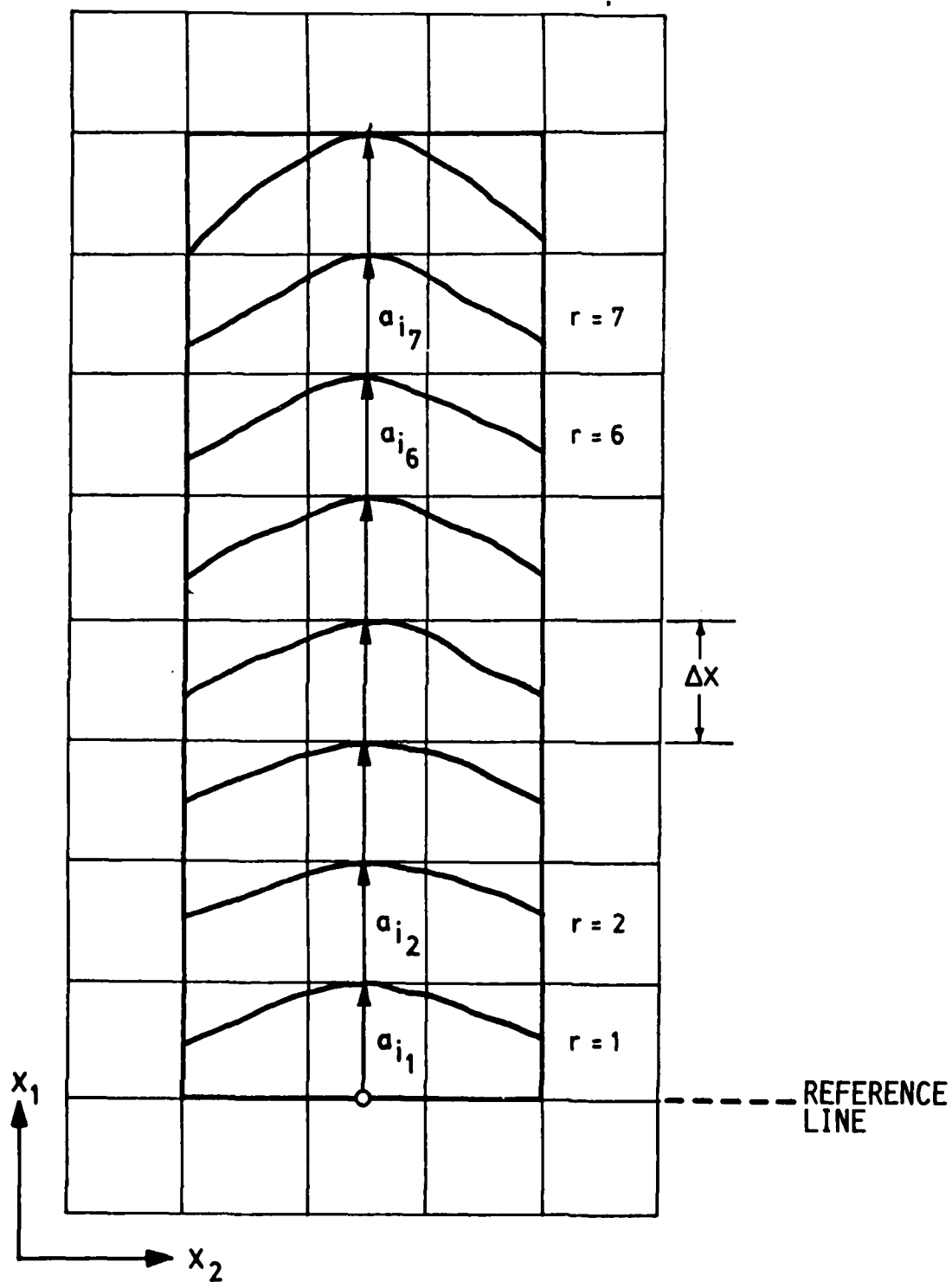
Figure 2: Schematic of the Proposed Fatigue
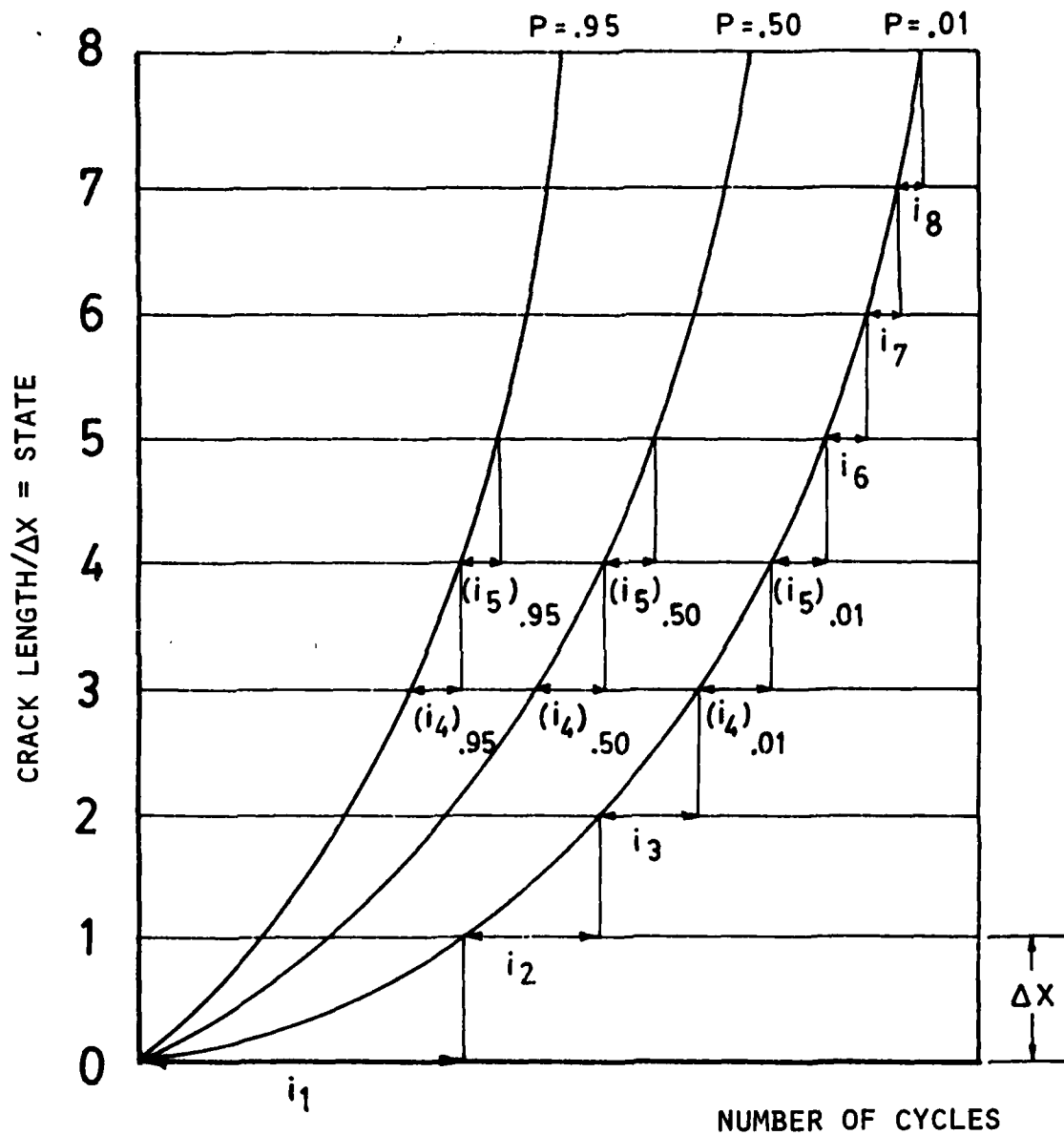Crack Propagation Model

Figure 3: Schematic of Constant-Probability
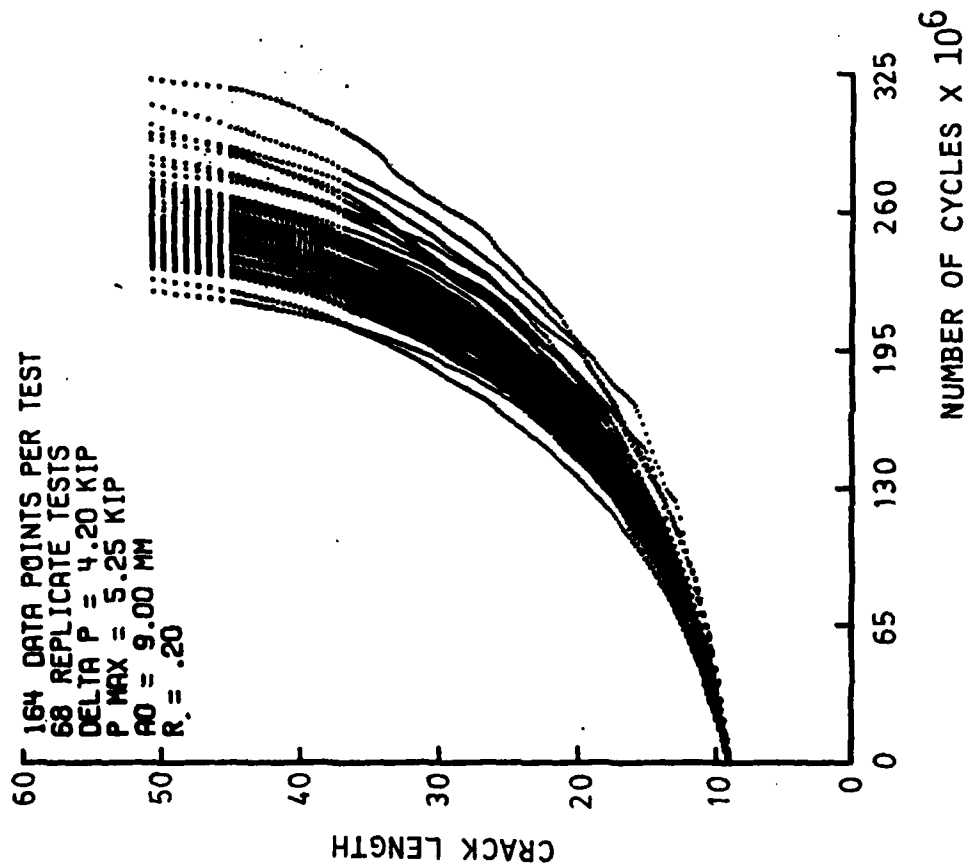Crack Growth Curves as Generated
by Equation (16)

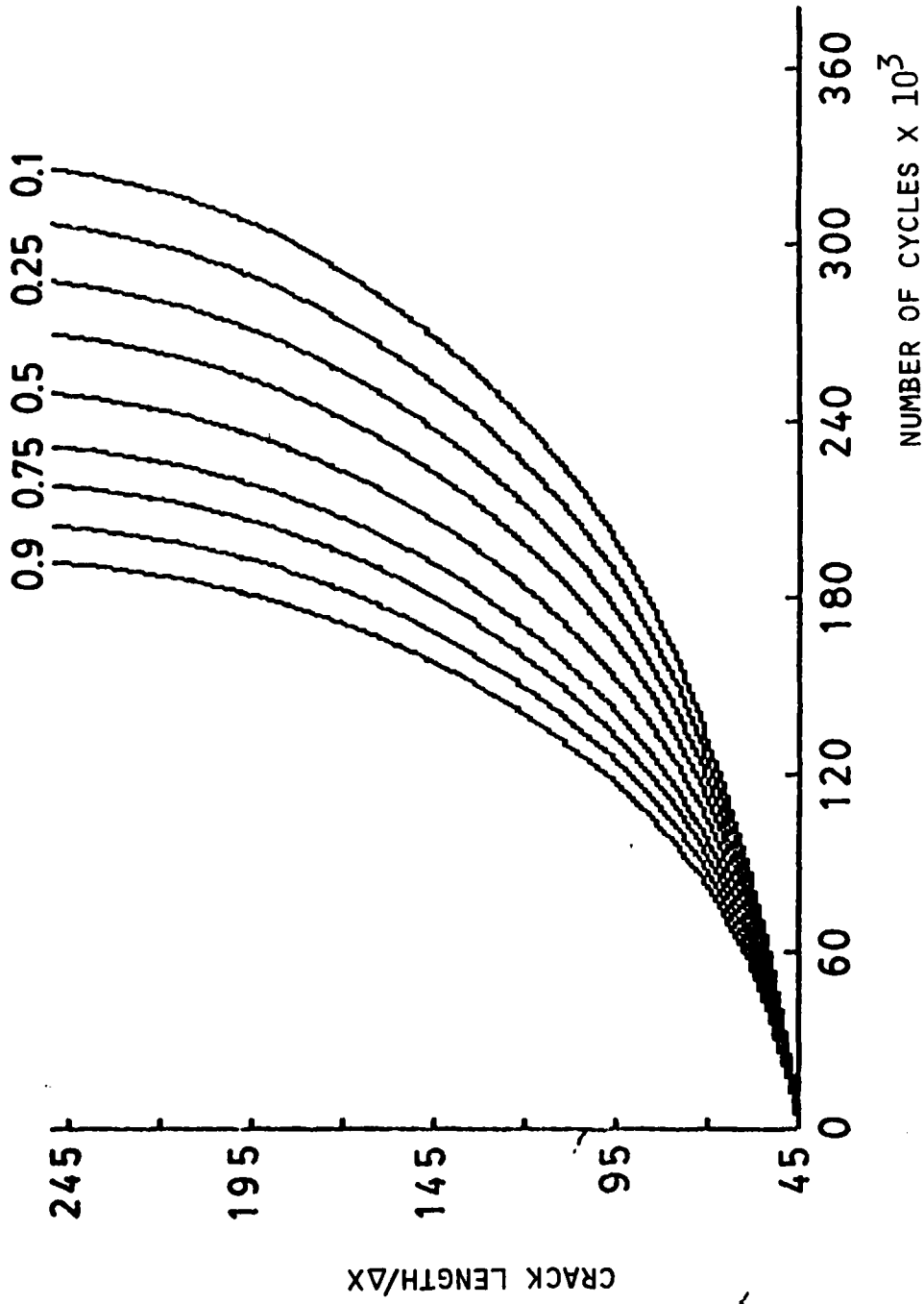Figure 4: Replicate a versus i data set
from Virkler's Study (15)

Figure 5: Experimental Constant-Probability Crack Growth Curves Generated From Data in Reference (15)
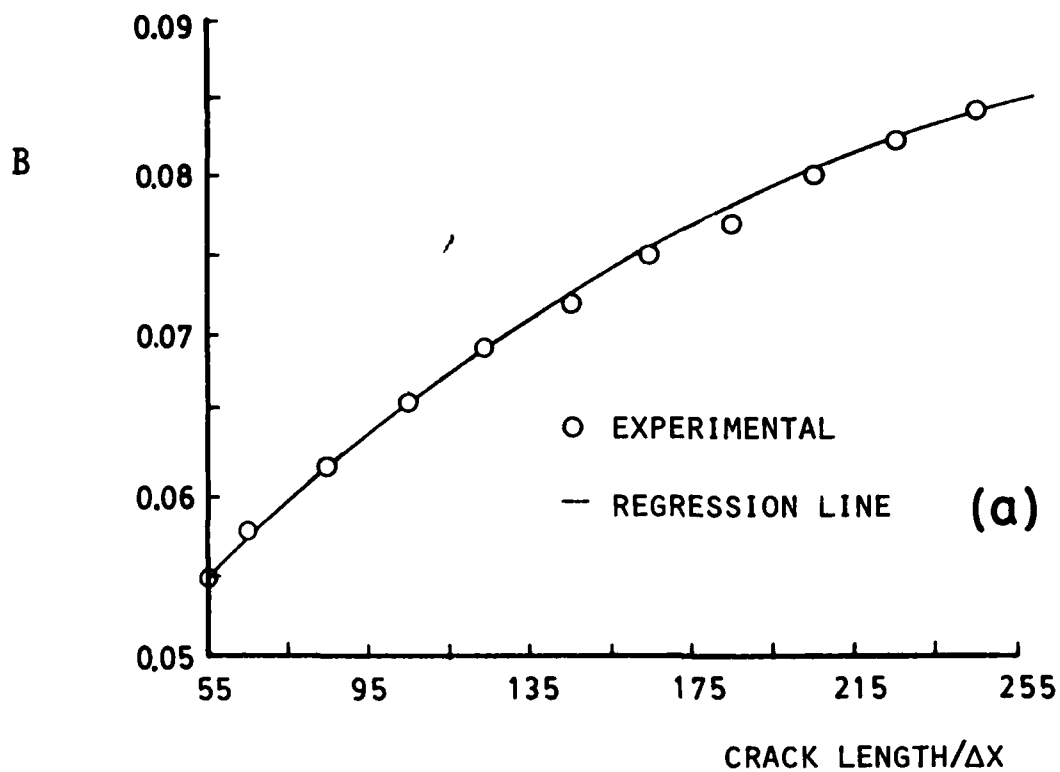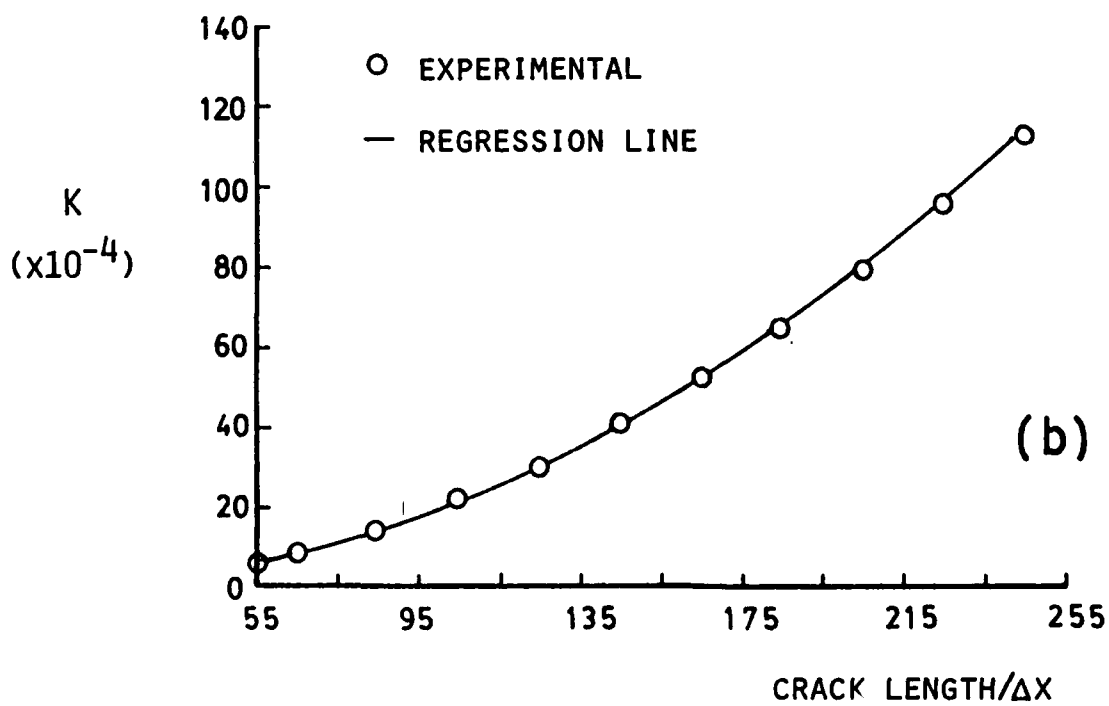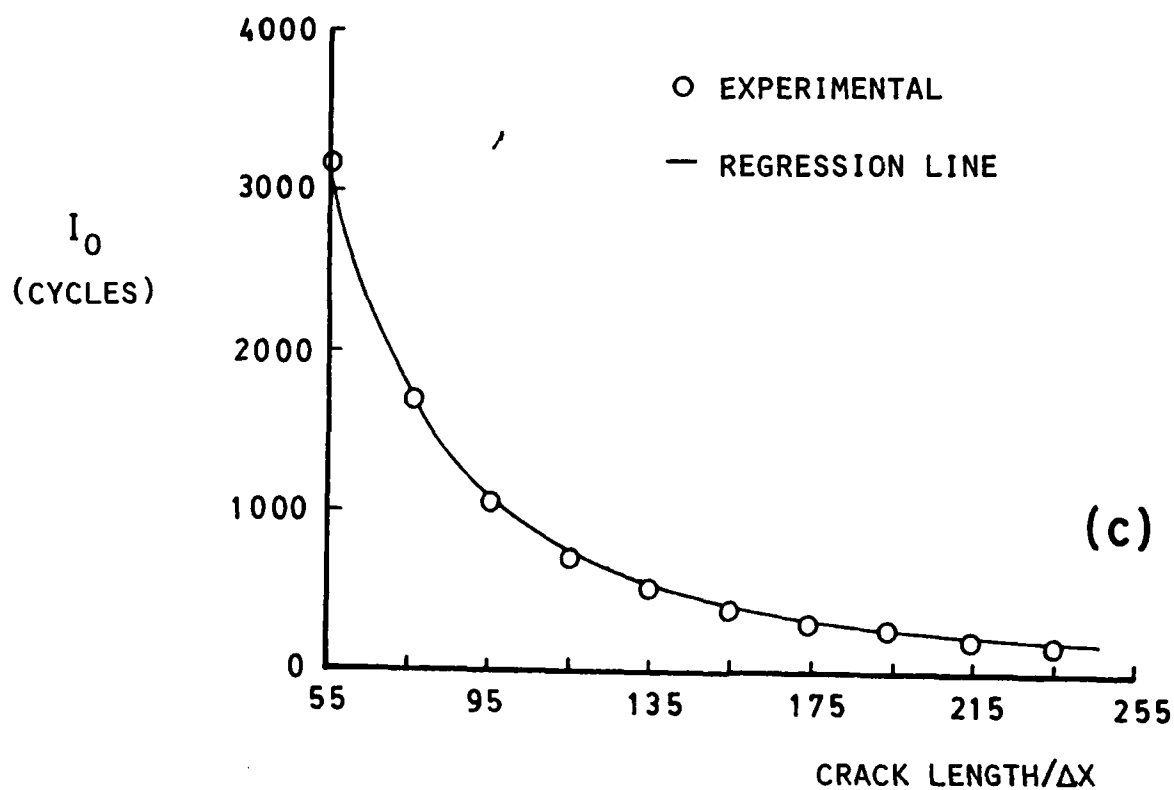
Figure 6(a)

Figure 6(b)

Figure 6(c)

Figure 6: Relationship Between B, K and I_0 and Crack Length Based on Experimental Data from Ref.(15).
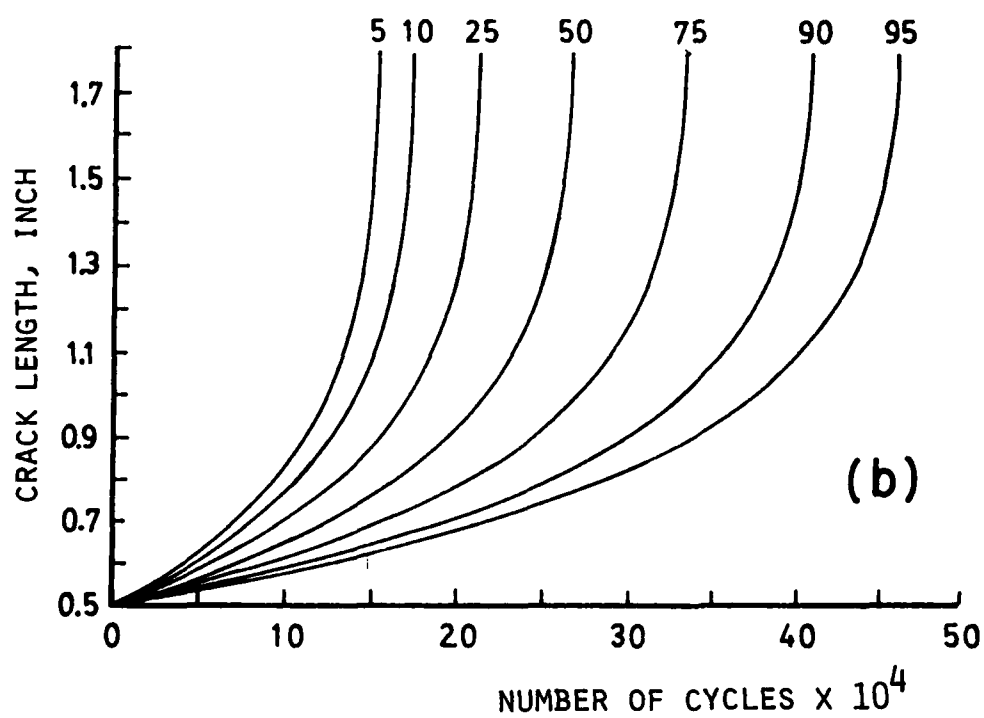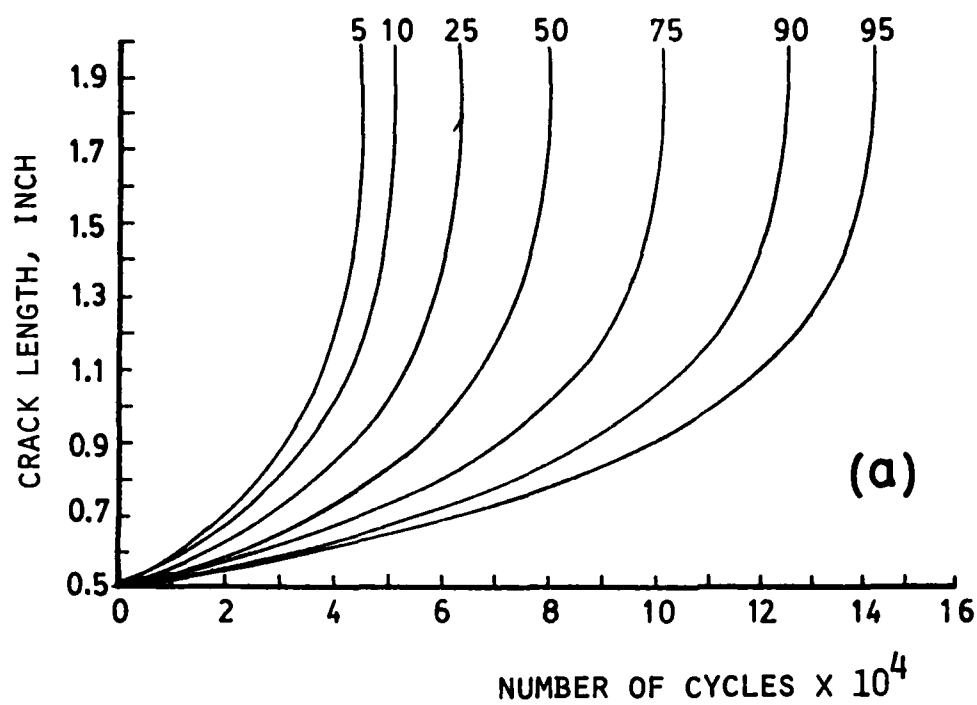
Figure 7:   Experimental Constant-Probability Crack Growth
            Curves for a) Test Condition I and b) Test
            Condition II (Ref.(16))
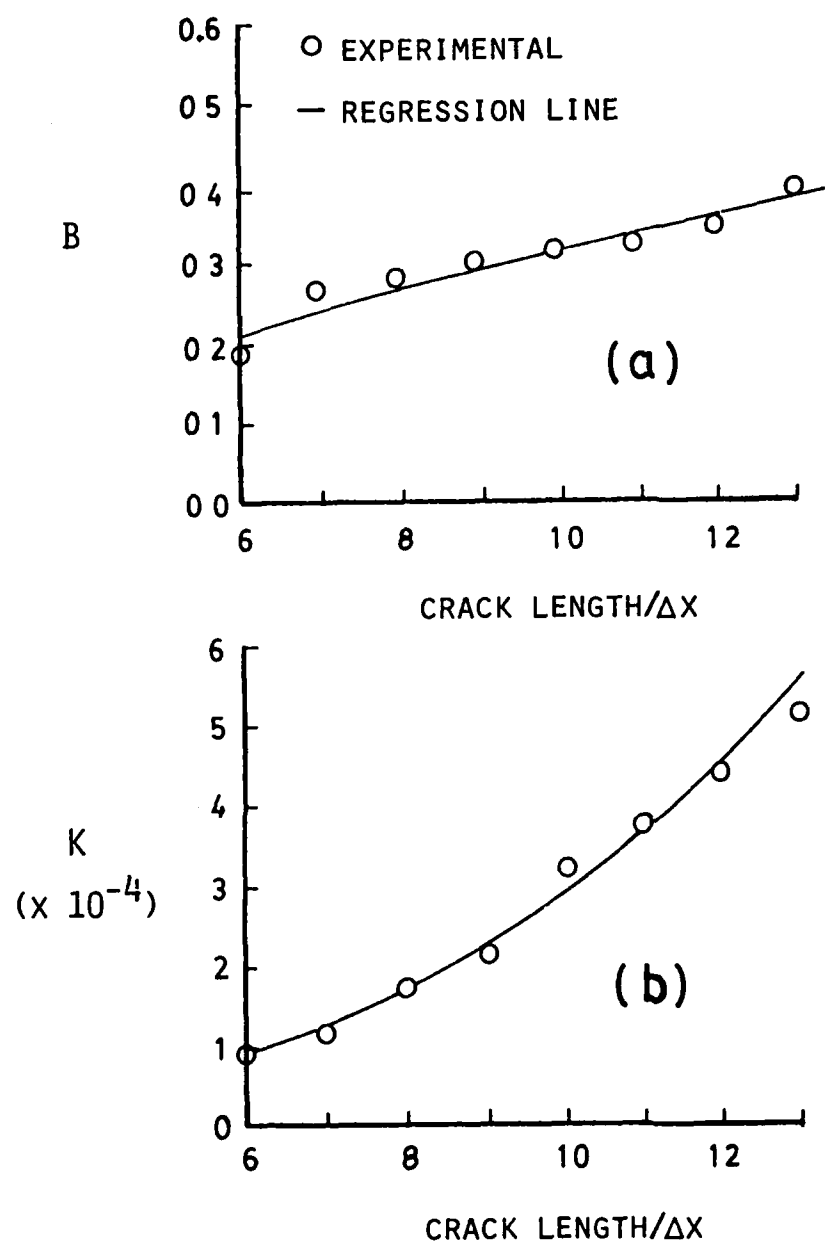
Figure 8(b)
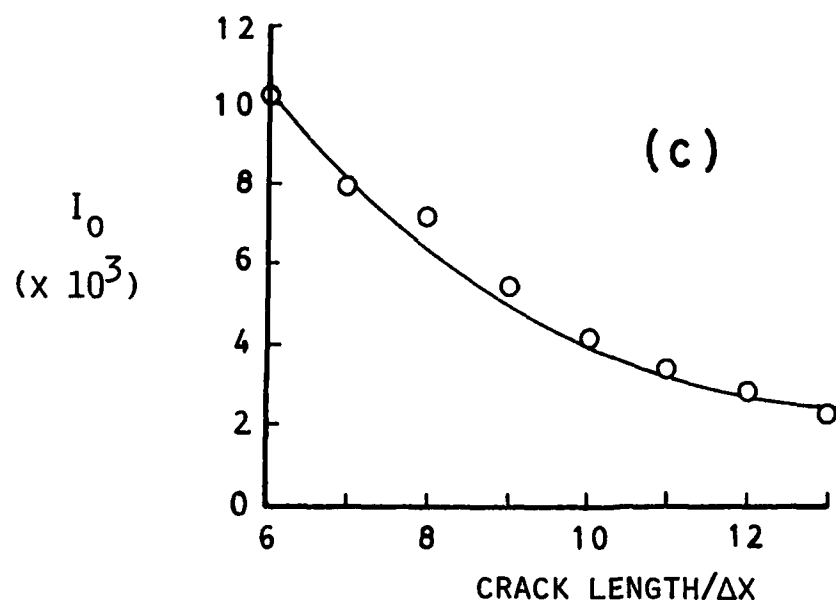
Figure 8(c)

Figure 8: Relationship Between B, K and I_0 and Crack Length Position for Test Condition I for Ref (16)
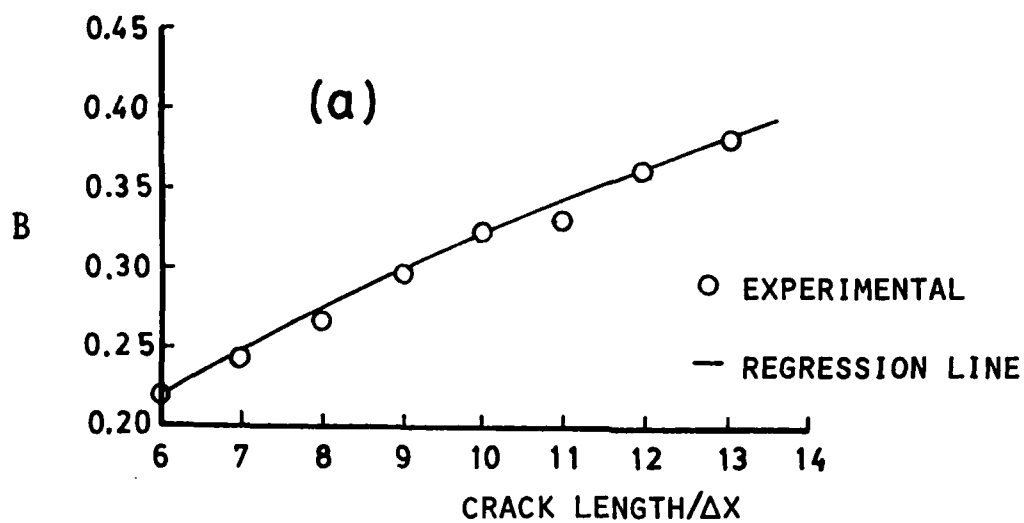
Figure 9(a)
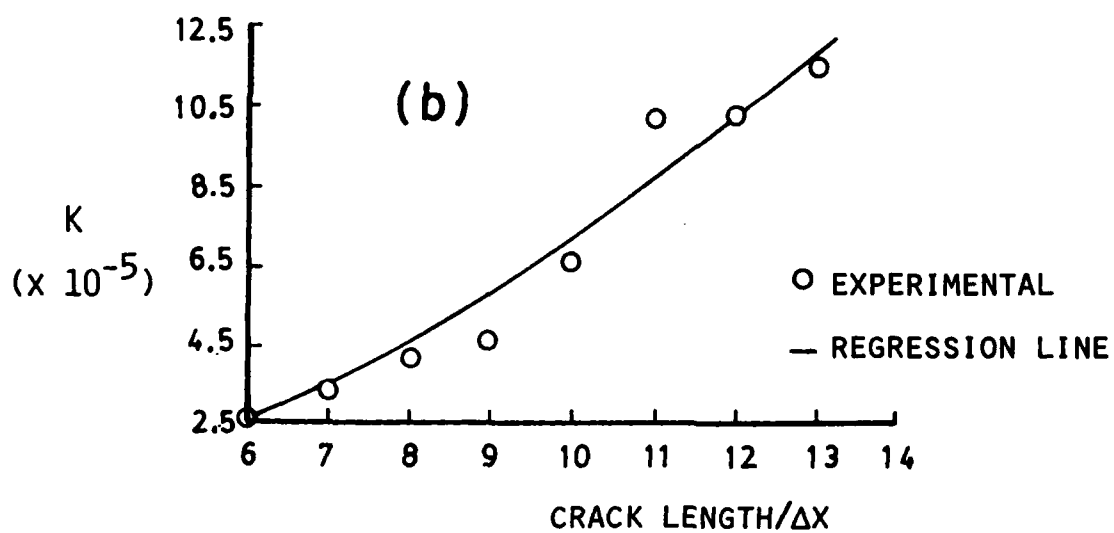
Figure 9(b)
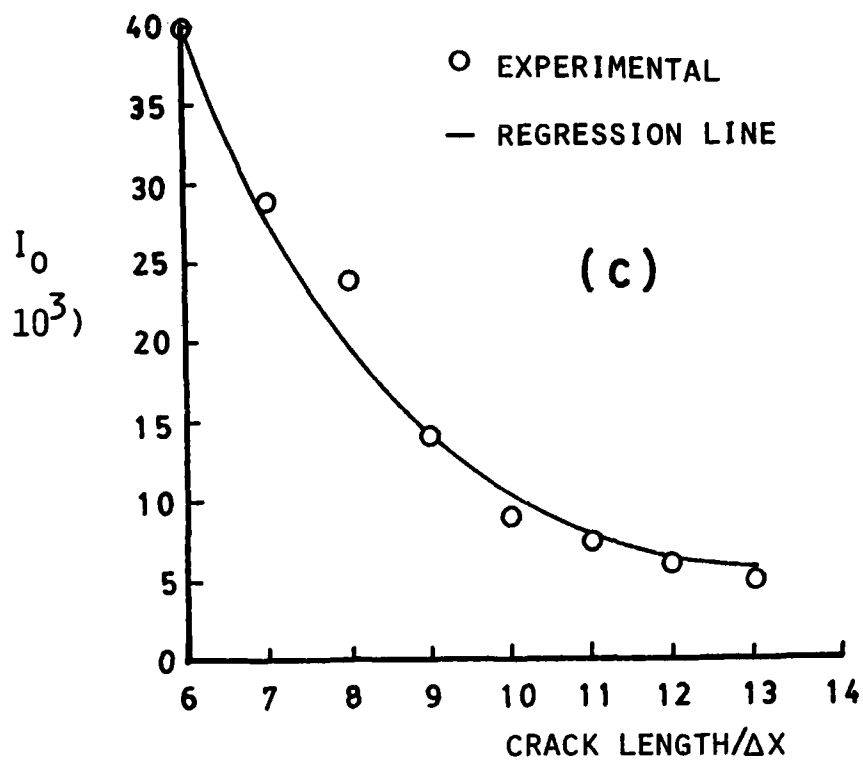
Figure 9(c)

Figure 9: Relationship Between B, K and I_0 and Crack Length Position for Test Condition II in Ref (16)
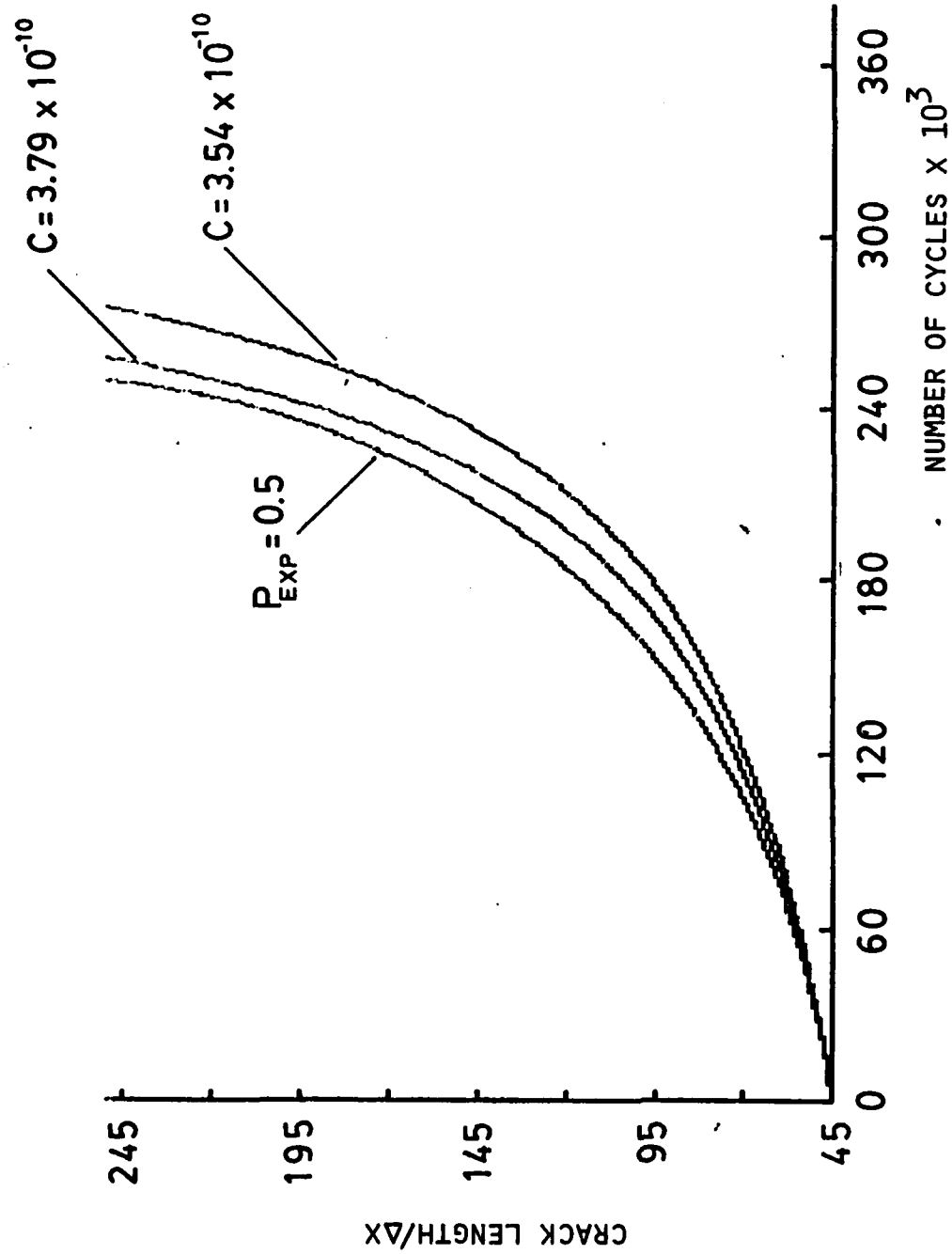
Figure 10: The Experimental Mean Crack Growth Curve ($P_r(i) = 0.5$) and the Corresponding Theoretical Curves Using the P-E Equation with Differenct C Values
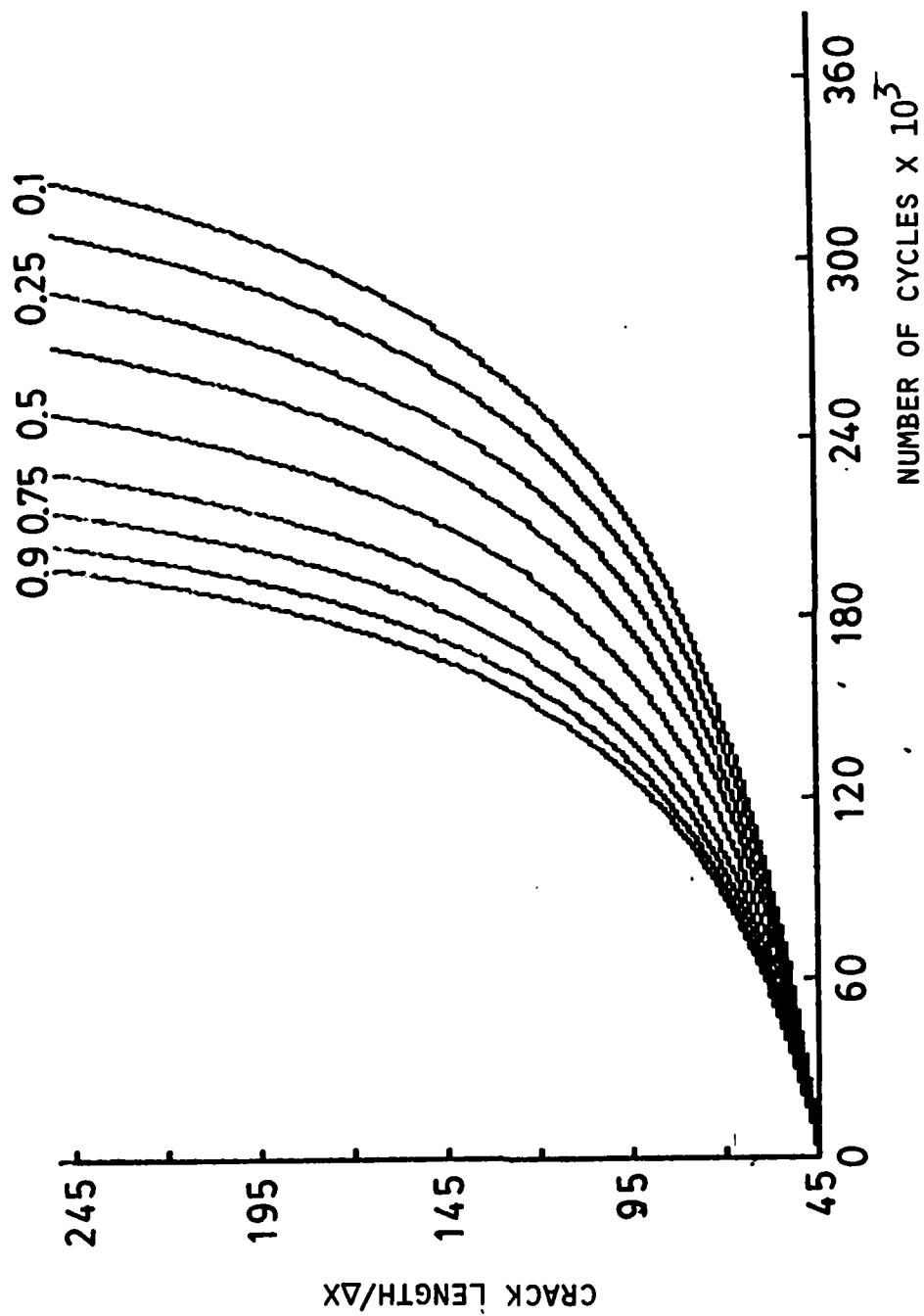
Figure 11: Theoretical Constant-Probability Crack Growth Curves Generated for the Test Condition Reported in Ref (15)
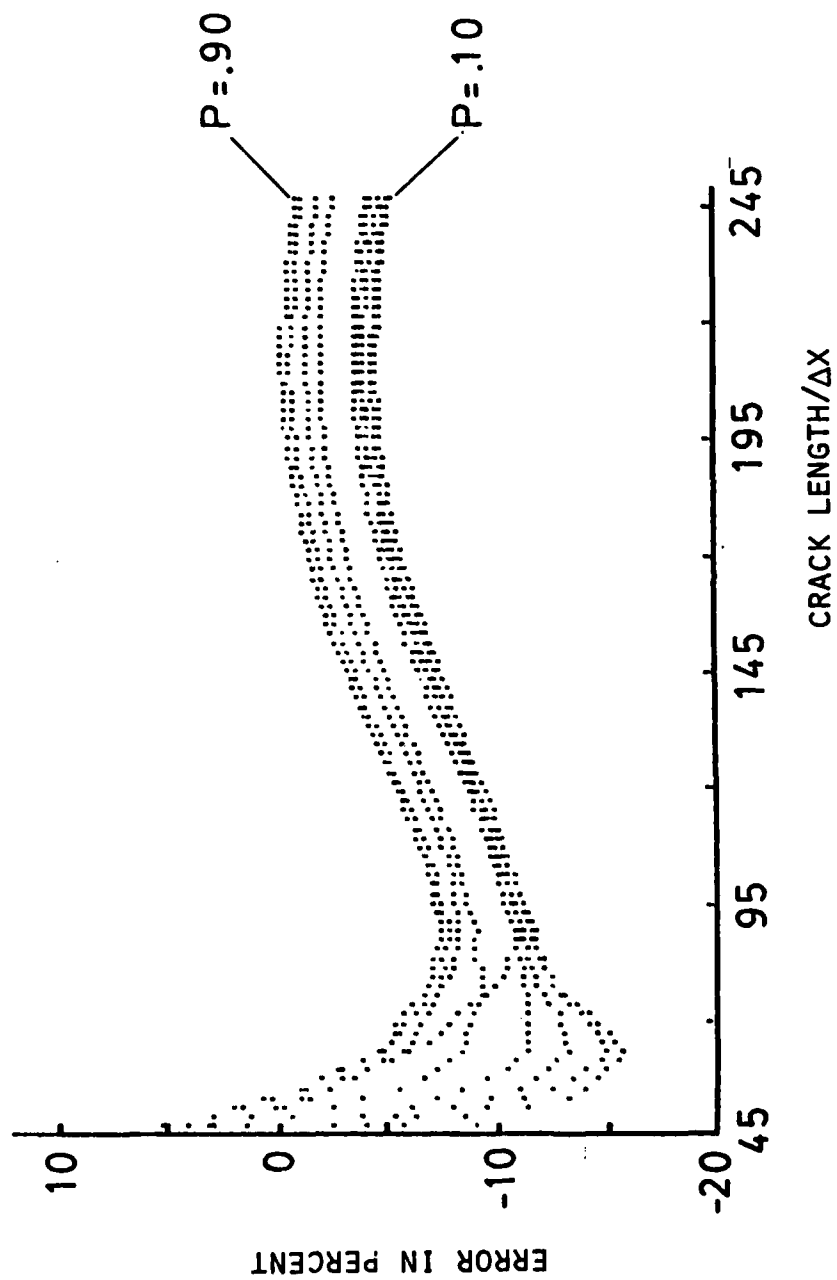
Figure 12: Error in Percent of the Proposed Model for C (in the Paris-Erdogan Equation) = 3.79x10⁻¹⁰

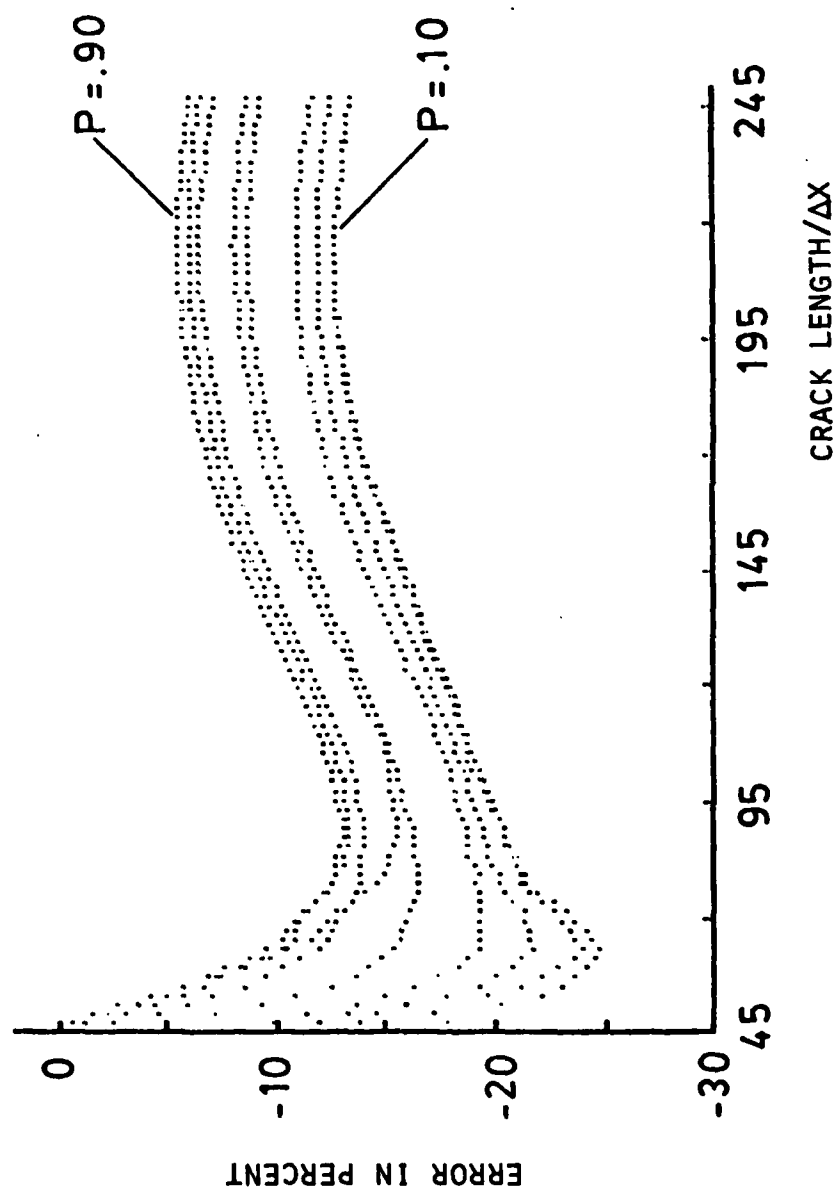Figure 13: Error (in Percent) of the Proposed Model for C in the Paris-Erdogan Equation) = 3.51 x 10⁻¹⁰
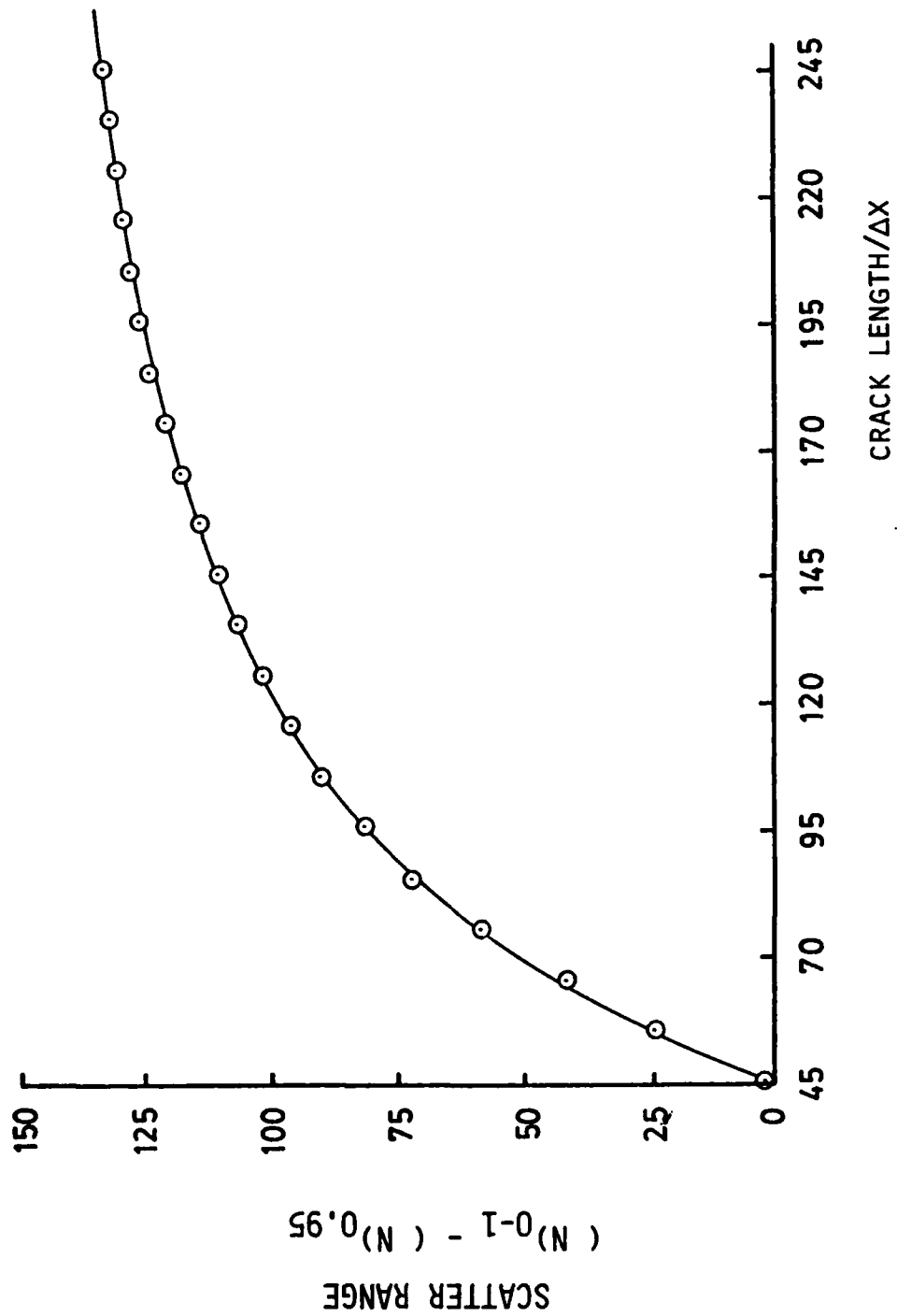
Figure 14: Variation of Scatter Range as Function
of Crack Length Position

END

FILMED

1-86

DTIC